Environmental Science
Processes & Impacts

Accepted Manuscript

ROYAL SOCIETY OF CHEMISTRY

rsc.li/process-impacts

The characteristic of PM2.5 in cities around the world has become a growing concern due to the extremely high concentration of these particles in many rapid expanding metropolitan areas. This study has determined the possible sources causing these high concentrations and analyzed the molecular composition of the ambient fine particulate matter in metropolitan Beijing. The study successfully combined TEM and multiple spectroscopic analyses (NMR, FTIR and Raman) to elucidate the molecular species with relatively good precision. The study confirmed the ability of non-destructive analysis methods to obtain useful conclusions on PM2.5 composition. Synchronized features were found among the TEM, NMR, FTIR and Raman spectra. These techniques may be beneficial for future particle research.

Environmental Science:
Processes & Impacts

RSCPublishing

ARTICLE

Characterization of Fine Particulate Matter in Ambient Air by Combining TEM and Multiple Spectroscopic Techniques ---- NMR, FTIR and Raman spectroscopy

Zhurun Ji,[a] Rucheng Dai[b] and Zengming Zhang[b*]

This paper reports a systematic study of the microstructures and spectroscopic characteristics of $PM_{2.5}$ and potential sources in Beijing by combining Transmission electron microscope and multiple spectroscopic techniques: Nuclear Magnetic Resonance, Fourier Transform Infrared and Raman spectroscopy. TEM images showed that dominant components of $PM_{2.5}$ are airborne organic substances with many trace metal elements which are associated with combustion sources. NMR spectra precisely determined the percentage of carbonaceous speciation in both $PM_{2.5}$ (with spatial and temporal distribution) and potential sources, and distinguished the similarities and differences among them. In FTIR spectra, a remarkable peak at 1390 cm^{-1} appeared only in $PM_{2.5}$ samples was attributed to NH_4NO_3, representing the occurrence of secondary processes. Raman spectra revealed certain inorganic compounds including the sulfate and nitrate ions. Based on the analysis of decomposition of Raman spectra, spectral parameters provided structural information and helped to find potential sources of $PM_{2.5}$. In the space of carbon aromaticity index and I_{D1}/I_G, $PM_{2.5}$ points followed a linear distribution which may also be useful in source tracing. The result shows that the combining non-destructive methods are efficient to trace the sources of $PM_{2.5}$.

1. Introduction

Particulate matter (PM) referring to the solids, colloids and droplets in the air is known as aerosols. Aerosol particles usually consist of many organic and inorganic compounds, of which carbonaceous matter (elemental and organic carbon due to the incomplete combustion of fossil fuel and biomass and the oxidation of biogenic volatile organic compounds)[1] is predominantly present in the submicron size fraction.[2-3] According to field monitoring, PM sizes have been classified into two groups, one at 10 μm and the other at approximately 0.1 μm. The increase of the fine particulate matter ($PM_{2.5}$, i.e., PM with aerodynamic diameters less than 2.5 μm) in ambient air could cause more frequent atmospheric visibility degrading fog, mist, haze or smog events[4] and also result in a greater damaging effect on public health, as many harmful substances are attached to the surfaces of fine particles.[5-7] $PM_{2.5}$ comprises a large variety of both primary and secondary particles (including secondary aerosols, combustion particles and condensed organic and metal vapors) that are dispersed throughout the atmosphere from a variety of sources.[8-9]

Generally, $PM_{2.5}$ originates from different sources or from different activities within the same source. For instance, it can be from natural processes (wildfires and volcanic dust, sea spray, pollen etc.), anthropogenic processes (including direct emissions, such as straw burning, vehicle exhaust (especially diesel exhaust), first and second hand smoke, and fumes from the kitchen), or chemical transformation processes of sulfuric acid droplets, sulfate, nitrate acid droplets and nitrate. The sources of $PM_{2.5}$ are so complicated that monitoring and tracing its sources in some cities (e.g., Beijing) becomes a difficult but key task.[10-20] However, the source emission particles (soot, the black solid product of incomplete combustion or pyrolysis of fossil fuels and other organic materials) are of particular concern, as they are hazardous environmental pollutants that account for a major fraction of $PM_{2.5}$ in urban areas. However, there are still great uncertainties about the chemical formation and origins of many potential soot species. Meanwhile, the chemical compositions of $PM_{2.5}$ that are related to emission sources and formation processes are quite complex.[21-22] Studying the chemical components and molecular structure of soot is important for many environmental factors; soot arises from a variety of potential sources of ambient air $PM_{2.5}$ (vehicle exhaust, fly ash and fumes) and is formed from many complex mechanisms involving reactive intermediates in the pyrolysis or combustion processes.[23-25]

$PM_{2.5}$ and soot particles are examined by a variety of methods, including some direct measuring methods (e.g., absorption, reflectance or gravimetric methods) and other indirect analysis methods (e.g., expensive and destructive or non-destructive methods). The traditional analytical approach of extraction and separation of the solvent-extractable (e.g., polar or nonpolar solvent, alcohol, water) materials from the samples can provide specific composition and quantification, but it has difficulty providing real-time data and also gives rise to positive or negative artifacts (e.g.,

through the adsorption of gas-phase products or evaporation of semivolatile organics).[26-28] To avoid the man-made interferences, researchers usually employ non-destructive analysis methods. The solid state ^{13}C-NMR can demonstrate the speciation of carbonaceous matter in the particle molecule.[29-30] Fourier Transform Infrared spectra (FTIR) have especially high selectivity, which is useful to provide information on the organic functional groups in particles.[31-32] Raman spectroscopy provides fingerprint spectra of each molecular species in organic and inorganic materials in the particle samples.[33-34]

In the last three decades, China has undergone very rapid economic growth, which has resulted in an increase of energy consumption, air pollution and associated health effects.[35-36] Sources of $PM_{2.5}$ in Beijing include fly ash, secondary sulfate, secondary nitrate, dust, coal combustion, vehicle exhaust, secondary ammonium, biomass burning, smoke and vegetative detritus.[15-16, 18, 37] The $PM_{2.5}$ components can reflect the predominant emissions of China, as well as the distinct local emissions, which indicates the significance of choosing the proper locations and measurement techniques for speciation monitoring. In this study, we report a systematic study on the morphology, composition, and molecular structure of $PM_{2.5}$ and the possible sources causing the high concentrations of those species in Beijing based on the combined use of TEM and various spectroscopic methods. The result indicates that combining multiple spectroscopic techniques is beneficial for the $PM_{2.5}$ analysis.

2. Experimental

2.1 Sample Collection

The sampling sites in this study are shown in Fig. 1. Information on the meteorological features of the sampling sites is provided below. The most serious haze-fog episode occurred in January 2013.[38] The temperature was generally between 10°C and 0°C in November 2012, between 0°C and -8°C in December 2012, and between 5°C and -10°C in January 2013. Home heating begins annually in mid-November in Beijing, causing a rapid increase of coal burning.

The particle samples were collected on quartz fiber filters (using high-volume samplers at a flow rate of 1.1-1.5 m^3/min and a sampling time of 24 h) from ambient fine particulate matter ($PM_{2.5}$). Particles from potential emission sources were also collected (using high-volume samplers at a flow rate of 1.1-1.5 m^3/min and a sampling time approximately 1.5-2 h), which included solid sources: diesel tailpipe particles (DTP), coal (honeycomb briquette, lump coal) and fly ash (furnace, stovepipe, kitchen chimney). Twenty-four-hour integrated $PM_{2.5}$ samples were collected at 5 downtown sites (sampled on January 17-28, 2013 during haze-fog episodes in Beijing, ref. 38) and 2 sites in the suburbs (sampled in November and December 2012). The potential emission source particles ($PM_{2.5}$) included vehicle exhaust (diesel and gasoline), smoke of biomass burning aerosols and anthracite coal collected on quartz fiber filters.

2.2 Sample analysis

The morphology and chemical composition of the samples were characterized by Transmission electron microscopy (TEM, JEOL model JEM-2000FX), which was equipped with an energy dispersive X-ray spectrometer (EDS, Oxford Link ISIS300). The EDS allows for semi-quantitative analysis of elements heavier than beryllium, except for Cu (The large Cu peak in the EDS map is due to the influence by the copper net for loading the sample). Quartz filter membranes (2.5 μm) and soot were placed in an ultrasonic oscillator filled with 20 mL ethanol for 20 min. Then, a drop of suspension was placed on the copper grid, dried in the open air for 10 min, and finally placed on the copper grid under TEM for analysis. EDS spectra of individual particles were obtained after scanning an electron beam with an accelerating voltage (with an operating voltage of 160 kV).

The collected samples were scraped from the filter membranes for analysis by NMR and FTIR techniques and were directly observed on the filter for Raman spectra analysis.

The NMR spectra is measured by ^{13}C NMR on a 600 MHz Bruker Avance NMR spectrometer with a solid-state 4 mm dual frequency MAS probe.

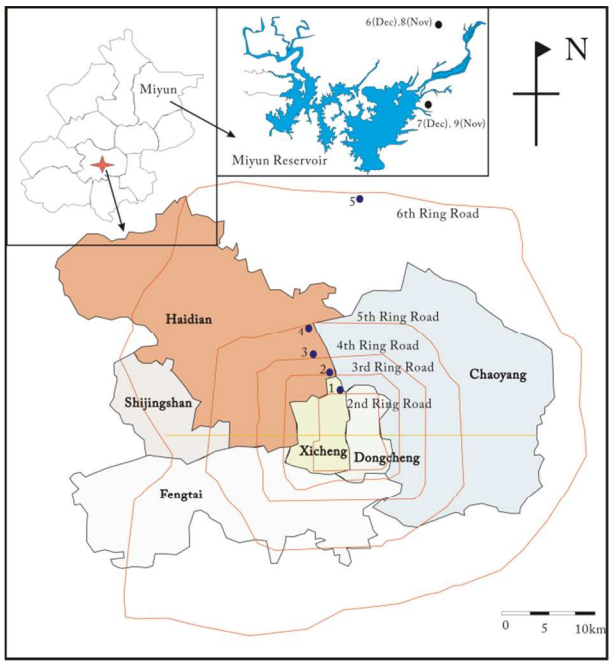

Figure 1 location of sampling sites in Beijing: samples 1-5 represent the second through the sixth ring roads in downtown Beijing; 6-7 represent Sihecun and Huanggezhuang, suburbs of Beijing (Miyun county) in December 2012; and 8-9 represent Sihecun and Huanggezhuang, suburbs of Beijing (Miyun county) in November 2012.

The FT-IR spectra of the samples were detected on a TENSOR-37. The Raman spectra were recorded using an integrated laser Raman system (LABRAMHR, Jobin Yvon) with a confocal microscope and a thermoelectrically cooled multichannel charge-coupled device (CCD) detection system. The 632.8 nm line of a He-Ne laser was used as the excitation source with the power below 10 mW.

3. Results and discussion

3.1 Analytical transmission electron microscopy.

The technique of TEM-EDS has been proposed as a possible method to make a tremendous contribution to ambient air particles. [39-41] TEM pictures of $PM_{2.5}$ samples are shown in Fig. S1a-h. The most important component in these particles was the airborne organic substances, the second one was associated with minerals such as gypsum, barite, calcite, siderite and other soluble salts, and the least important one included clay minerals and few silicate minerals. The two major sources of organic matter in particles were identified: biogenic detritus (plant wax, microbes, etc.) and anthropogenic emissions (oils, soot, etc.), as reported in ref. 41. Some trace metals (Pb, Zn, Ba, Cr, Fe, and Mn) are absorbed by the airborne organic particles. This phenomenon expressed that the deposition of metals is affected by the organic matters. The EDS images indicate that the trace metals in these particles are usually associated with nanoparticles that are rich in Fe and Mn, which is similar with the result that the majority of the trace metals hosted by particles are Fe and Ti oxides in aerosol particulates.[40] The morphology shows that the particles might be from secondary or combustion sources (Fig. S1e-h). The presence of gypsum ($CaSO_4$) authigenic pelletiod in particles has been considered a symbol of secondary processes and has been interpreted to indicate the partial transformation of calcite ($CaCO_3$) by acid aerosols.[42] The existence of spherulitic microbeads with silicate and barium aluminate has been attributed to combustion sources,[43] especially coal combustion. Additionally, the carbon ball that absorbed multiple metals (Mn-Fe-Zn-Pb) is likely to be related to automobile emission sources.

The TEM pictures of solid samples (fly ash, coal and DTP) are shown in Fig. S2a-h. The submicron and nanometer carbon particles, as well as such contained elements as Fe, S, Cr, and Ca, are the main components of the DTP. Coal combustion is a major source of some anthropogenic metals.[44] Fly ash is a residue generated from the combustion of coal, and the fly ash samples from the furnace and stovepipe represent nearly complete and incomplete combustion, respectively. The composition of fly ash varies according to the sources, methods of combustion and composition of the coal.[45] The former contained amorphous and crystalline particles (gypsum, calcite, quartz) and silicate microbeads, and the latter was associated with the clay minerals (illite, kaolinites), authigenic minerals (e.g., rutile) and molten slags (containing Fe, grossularite). The silicate microbeads are similar to cenospheres,[46] which are characteristic hollow silica-alumina glass spheres. In the coal samples (honeycomb briquette, lump coal), carbon particles with a small amount of clay (illite, kaolinites) and silicate minerals were found, as well as some metals (Cr, Fe, Zn, Sn, In) combined with sulfide and fluoride. Due to the heterogeneous nature of coal, quantitative calculations on the metals released during the processes of coal burning and transportation to the atmosphere are a challenge. The differences between the metal elements of the $PM_{2.5}$ and coal samples indicated that coal combustion was not the only source of it.

3.2 ^{13}C solid-state Nuclear Magnetic Resonance (NMR) spectra

NMR is unquestionably the most powerful technique to identify different functional groups in the organic materials of a sample.[47-48] The ^{13}C solid-state NMR spectra of all the $PM_{2.5}$ samples are shown in Fig. 2a-b. The peaks are generally assigned to aliphatic carbon (0-45 ppm), oxygenated aliphatic carbon (45-110 ppm), aromatic carbon (110-160 ppm) and carboxylic carbon (160-190 ppm), and their carbon content percentages are provided in Table 1. The table shows that the H- and C-substituted aryl carbons may account for more than 80% of the total aryl carbons, while the O-substituted aryl carbons account for less than 20%. As shown in Fig. 2a-b, the aliphatic carbon region exhibits a broad peak possibly resulting from a mixture of various paraffinic carbons. For most samples, the integrated area of this region has a percentage beyond 40% for aliphatic carbon. The peak at 30 ppm is usually attributed to methylene carbon according to previous studies.[49-50] The peak of the downtown $PM_{2.5}$ samples is at 30 ppm, and there is a weak peak at

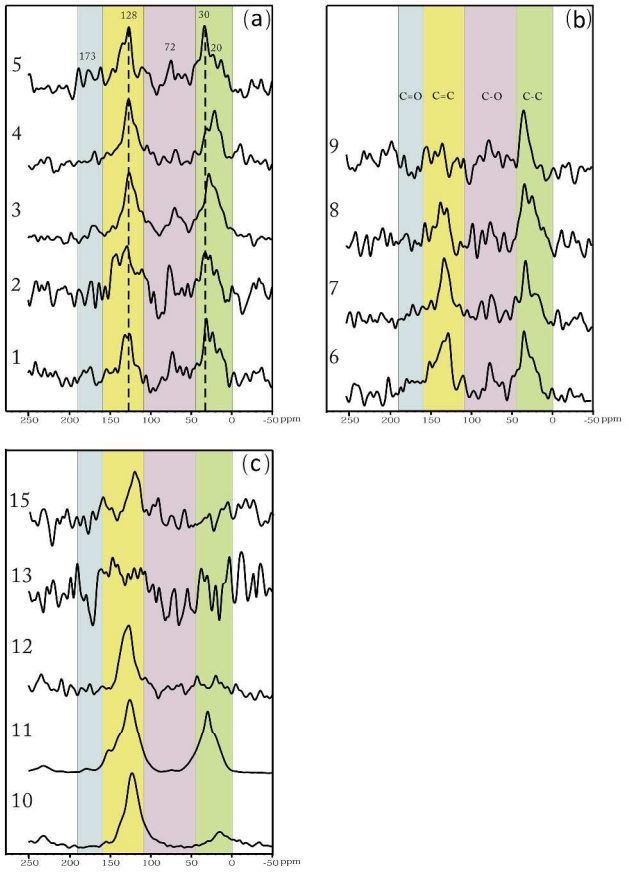

Figure 2 NMR spectra of $PM_{2.5}$ at (a) downtown sites, (b) suburban sites; (c) NMR spectra of solid samples (coal, fly ash and DTP). Samples 10-13 and 15 represent solid samples (honeycomb briquette, lump coal, fly ash of stovepipe, fly ash of furnace and DTP).

Table 1 Assignment and chemical shift of resonances (ppm) observed in the solid state ^{13}C-NMR spectra of $PM_{2.5}$ and solid samples. Integrated area (%) is shown.

Sample site and No.[a]		Aliphatic C 0-45	O-alkyl C 45-110	Aromatic C 110-160	Carboxylic C 160-190
Urban	1	57.3	7.9	34.8	0
	2	31.7	7.0	61.3	0
	3	47.4	9.3	41.1	2.2
	4	44.3	0	55.7	0
	5	49.8	6.6	38.5	5.1
Suburb	6	43.7	9.65	44.8	4.0
	7	44.5	5.6	46.6	3.3
	8	61.7	7.6	30.7	0
	9	52.4	22.7	13.2	11.7
Solid Samples	10	15.7	0	84.3	0
	11	42.2	0	57.8	0
	12	12.2	0	87.8	0
	13	20.6	0	72.6	6.8
	15	10.0	12.7	63.1	14.2

a) The carbon percentage values from the integrated areas are in %.

20 ppm in some samples (although for sample No. 4 whose sampling location is the Olympic Forest Park, it is very strong), which represents the aliphatic carbons in alkyl chains (-CH_3). The result of high aliphatic C components is predominantly due to combustion sources.[30] The TEM analysis also supports this conclusion (Fig. S1e, f). In the O-alkyl region, a strong signal at 72 ppm corresponds to alcoholic groups. In the aromatic C region, a strong signal at 128 ppm, along with a shoulder peak at 135 ppm, was observed. Specifically, the peak at 128 ppm dominates this whole region and can be attributed to a C ring of carbohydrates.[51] The carboxylic carbon region accounts for a small proportion of C components. It ranges from 0-5.1% for $PM_{2.5}$ in the downtown samples and 0-11.7% for the suburb samples. Amides and esters may contribute to the peak at 173 ppm, which is present only in some of the $PM_{2.5}$ samples.[52] The downtown sample results show that are same as that of the suburb sample in December, but the percentage of aromatic C is higher and that of aliphatic C is lower for the samples in December compared with those in November.

The ^{13}C solid-state NMR spectra of solid samples (fly ash, coal and DTP) are shown in Fig. 2c. The NMR spectra of coal samples are similar with spectra of the Everglades peat and the Brandon lignite (bedded coal up to the rank of bituminous coal).[53] For lump coal, both aromatic and aliphatic carbons are dominant components. For honeycomb briquette, the peak in aliphatic carbon region is too small to be discerned, which might be due to its manufacturing process. The spectra characteristics of the fly ash samples have similarities with those of unburned coal samples. The comparison between spectra of stovepipe fly ash and coals shows that after the combustion processes, the peak of aliphatic carbon may almost disappear. Furthermore, in comparison with the fly ash sample from the stovepipe, the fly ash sample collected from the furnace underwent more complete combustion processes, and the aromatic carbon peak is much smaller. The phenomenon indicates the decreases of both aliphatic and aromatic carbon during combustion. Unlike coal combustion samples that have no peaks in two regions, the spectrum for DTP has discernible peaks in both the O-alkyl and the carboxylic C regions, which is similar with $PM_{2.5}$. Consistent with earlier reports, DTP can be regarded as one of the most important sources of air particles,[54] especially the source providing O-alkyl C and Carboxylic C. All of the solid samples have much higher percentages of aromatic C than that of $PM_{2.5}$, indicating the existence of other Aliphatic C providers.

3.3 Fourier Transform Infrared (FTIR) spectroscopic analysis

The infrared spectra of all the $PM_{2.5}$ samples are shown in Fig. 3a-b. The exhibited peaks are similar with each other among most $PM_{2.5}$ samples from the downtown sites and the November and December samples from the suburban sites. It suggests that the structural and functional groups in the $PM_{2.5}$ samples have much similarity. The notable peak at 1630 cm^{-1} is attributed to aromatic C=C bond vibration.[31, 55-57] A large, sharp peak at 1390 cm^{-1}, which is not discernible in any of the spectra of potential sources (Fig.3c-d), and was ignored by some previous studies, is attributed to the NH_4NO_3.

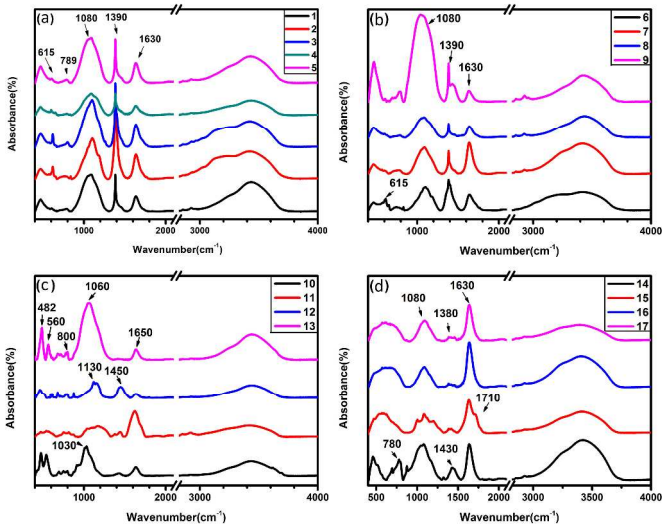

Figure 3 FTIR spectra of $PM_{2.5}$ sampling at (a) downtown sites, (b) suburban sites; FTIR spectra of (c) solid samples (coal, fly ash), (d) emission sources and DTP (Samples No. 14-17 represent fly ash of kitchen chimney (biomass burning), DTP, diesel vehicle exhaust and smoke of anthracite combustion. Other samples are the same as Fig. 2.)

compound.[58] It is on the behalf of the secondary particle which could be produced in the photochemical smog processes, and shows a high concentration of secondary particles. Interestedly, this result is in accordance with the conclusion of high secondary aerosol during haze events in Jan 2013, Beijing.[59] However, the intensity of this peak is significantly different from the $PM_{2.5}$ samples in November (samples No. 8, 9) and December (samples No. 6, 7), which is in accordance with the NMR spectra results. Additionally, all $PM_{2.5}$ samples have a broad peak at 1080 cm^{-1}. Some authors linked that

peak to the C-O bond vibration or polysaccharide substances alone,[60] but others believe that there is a strong overlapping with the sulfate ion peak at 1090 cm^{-1}. Most of the $PM_{2.5}$ samples have a peak at 615 cm^{-1}, which is another peak of SO_4^{2-},[23, 61] revealing that the sulfate ion is an important component of $PM_{2.5}$ particles.

The infrared spectra of emission source particles and solid samples (fly ash, coal and DTP) are shown in Fig. 3c-d. The solid sample for lump coal presented prominent peaks at 1650, 1450 and 1130 cm^{-1}, while the honeycomb briquette had a strong peak at 1030 cm^{-1} and two weak peaks at 1650 and 1450 cm^{-1} (Fig. 3c). The infrared spectra also display resemblances between the fly ash and unburned coal samples, the same as with the NMR analysis. The peak at 1450 cm^{-1} from the solid samples was remarkably different from the $PM_{2.5}$ peaks, which can be attributed organic functional groups, such as aliphatic carbon (-CH_3), acetone and methanol fractions (1300-1500 cm^{-1}),[56] CH_2 and CH_3 bend, and some aromatic ring modes.[62] Although similar, we still observed some differences between the DTP and $PM_{2.5}$ from their spectra. For example, the two shoulder peaks on the both sides of the 1080 cm^{-1} peak and an apparent shoulder peak at 1710 cm^{-1} attributed to the C=O bond vibration are not observable in the $PM_{2.5}$ samples. The potential emission sources share similar absorption spectra characteristics with that of DTP. The spectra of particles from potential emission sources have an obvious peak at 1630 cm^{-1}, a weak peak at 1380 cm^{-1} and a wide peak at 1080 cm^{-1}, just as with the $PM_{2.5}$ samples, except for a peak at 1430 cm^{-1} from the fumes of a biomass burning smoke sample. This finding exhibits great consistency in functional properties with $PM_{2.5}$.

3.4 Raman analysis of $PM_{2.5}$ on quartz fiber filter

Raman spectra for $PM_{2.5}$ are shown in Fig. 4a-b. The two known bands in the $PM_{2.5}$ samples at 1330 cm^{-1} and 1580 cm^{-1} are similar to the standard graphitic band (especially activated carbon).[24-25, 63, 74] Raman spectroscopy could not only provide characteristics of carbonaceous matter but also those for inorganic compounds. Between 900 cm^{-1} and 1100 cm^{-1} in the Raman spectra for the $PM_{2.5}$ samples, there are many small peaks (Fig. 4a-b). Some samples have a small peak at 1012 cm^{-1}, which is attributed to the sulfate ion (SO_4^{2-}).[64] The double peaks at 1018 cm^{-1} and 990 cm^{-1} for some samples are attributed to $(NH_4)_2SO_4$.[65] A sample (No. 8) has a peak at 1055 cm^{-1}, which is related to secondary inorganic compounds $Ca(NO_3)_2{\cdot}4H_2O$ or $NaNO_3$.[66] The conclusion is accordance with the TEM analysis (Fig. S1b, h) and FTIR analysis (Fig. 3a).

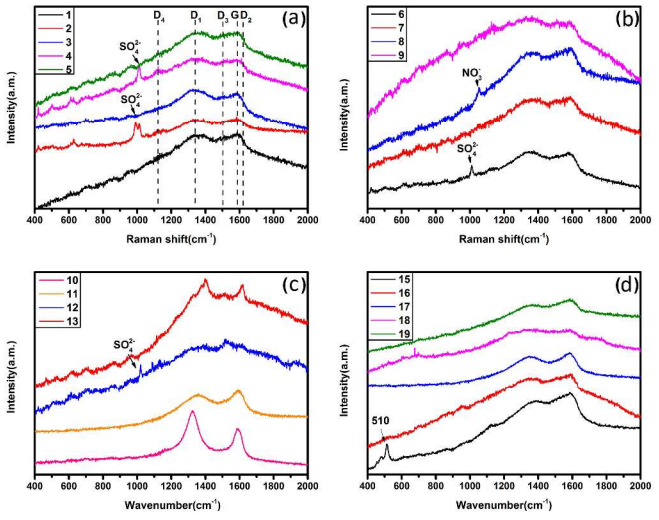

Figure 4 Raman spectra of $PM_{2.5}$ at (a) downtown sites, (b) suburban sites; Raman spectra of (c) solid samples (coal and fly ash), (d) DTP and emission sources. (Sample No. 18-19 represent gasoline vehicle exhaust and smoke of biomass burning collected on quartz filters. Other samples are the same as Figure 3.)

The nitrate ion (NO_3^-) is mainly produced by automobile exhaust, and the sulfate ion (SO_4^{2-}) mainly originates from coal in the Beijing area.[67] These two pollutants – nitrate and sulfate ions – might not be directly emitted from the sources but derive from a chemical transformation process in the atmospheric particles. In addition, most samples have insignificant small peaks between 500 cm^{-1} and 1100 cm^{-1}, such as the weak peaks at 510 cm^{-1} and 857 cm^{-1} (sample No. 2), at 628 cm^{-1} (sample No. 4), and at 698 cm^{-1} and 948 cm^{-1} (samples No. 1, 3, 5).

Raman spectra of emission source particles and solid samples (fly ash, coal and DTP) are shown in Fig. 4c-d. The solid coal samples presented typical "graphitic" spectra, but the widths and relative intensities of two bands, which describe the structure order of the sample, are different between lump coal and honeycomb briquette.[33] The small peak at 1020 cm^{-1} from the fly ash samples should be attributed to the sulfate ion (SO_4^{2-}) (Fig. 4c), while no peak appeared in this inorganic matter area for the DTP and emission source samples (Fig. 4d). These spectra do not obviously differ from that of the $PM_{2.5}$ samples. Peaks appearing at 291, 373, 454, 480 and 513 cm^{-1} for the DTP sample indicate that iron minerals (e.g., goethite, hematite) are in the soot.[68] In addition, weak peaks at 614, 698, 866, and 966 cm^{-1} also confirm the iron minerals (e.g., scorodite, yukonite) in this sample.[68] The TEM results support this analysis.

In this research, the Raman spectra of $PM_{2.5}$ samples are decomposed with 4 Lorentzian bands and 1 Gaussian band, five bands G, D1-D4 at approximately 1580, 1350, 1620, 1500 and 1200 cm^{-1}. The result of five-band fitting is shown in Figure S3; the band parameters, including band positions (Stokes shift, cm^{-1}), full width at half-maximum (FWHM, cm^{-1}) and integrated band intensity ratios between D1, D2, D3 and G, are summarized in Table S1.

The carbonaceous matter in $PM_{2.5}$ can be divided into amorphous carbon and crystalline carbon. D3 band (~1500cm^{-1}) can be attributed to the amorphous carbon, such as organic molecules and functional groups. The decomposed spectra shows that the amorphous carbon takes up a smaller proportion in $PM_{2.5}$ than in most sources and the content is closely related to the amorphous carbon content of the main sources. The accurate ratio of amorphous carbon to crystalline carbon can be determined by scaling of Raman spectra in further study and improve the cognition of carbonaceous matter in $PM_{2.5}$.

3.5 Source analysis

In NMR measurement, carbon aromaticity index *fa* represents the ratio of aromatic carbon to total carbon. I_{D1}/I_G in Raman spectra is also an important parameter reflecting the abundant graphite structure (or the structure order in the view of crystallography).[24-25] As shown in Fig. 5, there is a negative linear relationship between the carbon aromaticity index *fa* and the parameter I_{D1}/I_G for $PM_{2.5}$ samples. The linear correlation coefficient is 0.86. Also, the points of solid samples are partly at one end of this correlation line. According to the two end-members mixing model, there is definitely another source which has a low fa and a high I_{D1}/I_G value. This line may give some guidance to the search of sources in Beijing and furthermore, beneficial in source tracing.

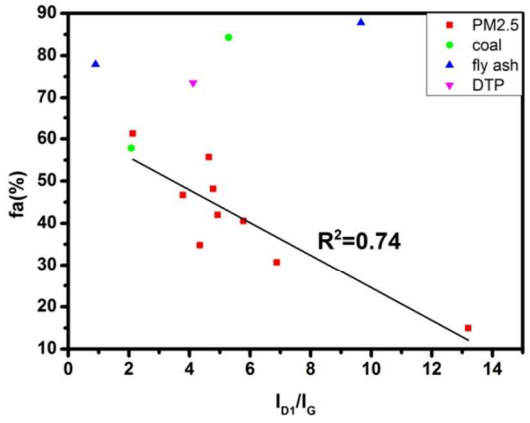

Figure 5 Relationship between the carbon aromaticity index in NMR spectra and a carbon curve fitting parameter (I_{D1}/I_G) in Raman spectra of $PM_{2.5}$ and solid samples.

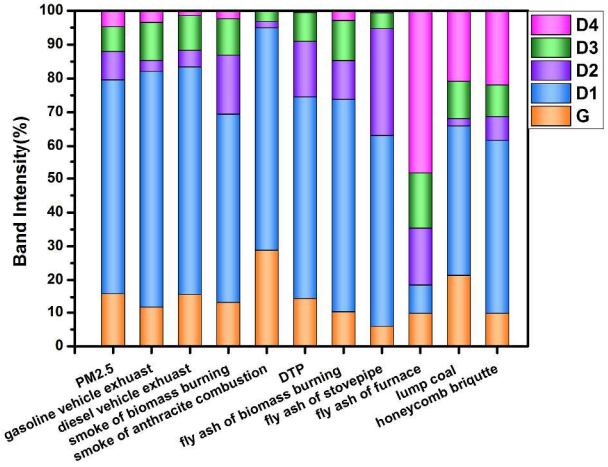

Figure 6 Relative intensities of the D, G1, G2, G3 and G4 band from $PM_{2.5}$, solid samples and emission source samples obtained from the curve fitting as in Fig. 5. The first group of columns are the average intensity values of $PM_{2.5}$ samples (error bars represent for the standard deviation), and other groups are the band intensities of potential sources.

In Fig. 6, the band intensities of $PM_{2.5}$ samples are very similar with that of potential emission sources, DTP and fly ash of biomass burning, but are very different from other solid samples (coal, honeycomb briquette, chimney fly ash and furnace fly ash). It can be inferred that $PM_{2.5}$ samples and coal and fly ash samples have quite different components and structures. So as a conclusion, oxidation is an important process in $PM_{2.5}$ generating. Some researchers have identified the phenomenon of the G peak blue shift in the oxidation process of soot, [69] which meet the characteristics of the Raman spectra of the furnace fly ash sample (long time at high temperature, approximately complete combustion) in this study. The G peak shifted from 1580 cm^{-1} to 1615 cm^{-1}, and the D1 and D2 bands are also blue shifted. Moreover, the half peak width of the D1 band and I_{D1}/I_G of the furnace fly ash sample are at the minimum values among the various sources (Table S1), illustrating that the heterogeneity of the fully oxidized ashes is very low. In addition, several papers reported that the D4 band might disappear in the oxidation process from approximately 1200 cm^{-1} and move near 1120 cm^{-1} in the spectra of DTP.[70] In this study, for most of the $PM_{2.5}$ samples, the D4 band appeared at approximately 1120 cm^{-1}, the same as the emission sources while D4 band appeared at 1200cm^{-1} in most of solid samples. These results are considered to be due to particle oxidization in emission process and in ambient air, such as thermal processes that lead samples to contain more sp^3 hybridized carbon material. This characteristic divides sources into indirect ones and direct ones.

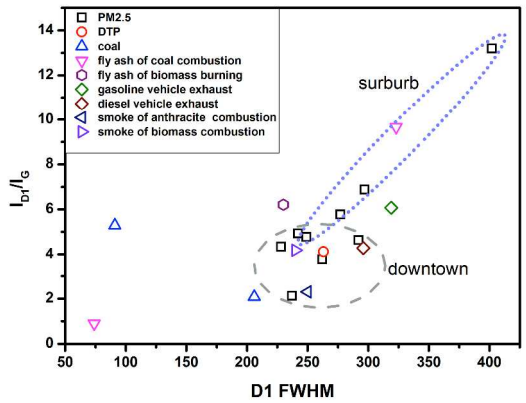

Figure 7 Spectral parameters of different $PM_{2.5}$, solid samples and emission sources samples. Integrated band intensity parameters I_{D1}/I_G vs. the half peak width (FHWM) for $PM_{2.5}$ and all potential sources.

Figure 7 shows scatters of D1 FWMH with the intensity ratio I_{D1}/I_G of $PM_{2.5}$ and potential source samples. Considering the coordinate positions of these samples in this graph, it can be observed that the points of the $PM_{2.5}$ samples in downtown are distributed in a limited region, and are quite close to the potential sources (e.g., DTP, smoke of biomass burning, smoke of anthracite combustion and diesel vehicle exhaust), and some solid sources (lump coal and fly ash of biomass burning) are also near to the region. However, the points of the $PM_{2.5}$ samples in suburbs are distributed in a straight line and the

point of stovepipe fly ash is on this line. Specifically, one end member of the line (the $PM_{2.5}$ sample in December) is close to the region (the $PM_{2.5}$ samples in downtown), as suggested by the NMR, FTIR and Raman results.

5. Conclusions

Combining TEM and multiple spectroscopic methods can be used to investigate the composition and molecular structure of original samples for fine particulate matter ($PM_{2.5}$) in ambient air and potential source. The results from these methods can be confirmed by each other. In this study, TEM observation found three types of components in $PM_{2.5}$, dominantly airborne organic substances and absorbed trace metals, which is mainly derived from combustion sources. The sources of organic matter in particles, biogenic detritus and anthropogenic emissions, can be identified. NMR spectra can provide the precise percentage of the different carbonaceous speciations in $PM_{2.5}$ and show that aromatic C and aliphatic C are the predomination. FTIR spectra identify the existence of secondary particles and the main carbon bonds including the aromatic C=C bond, aliphatic C-H bond and C-O bond in $PM_{2.5}$. Raman spectroscopy can precisely index the potential sources of carbonaceous matter and easily finds the existence of inorganic matters, SO_4^{2-} and NO_3^- in $PM_{2.5}$. The aromaticity charactered by NMR spectra and fitting parameters in Raman spectra can be important indicators of sources.

This study shows that non-destructive methods have efficiency to trace the sources of $PM_{2.5}$. They can be further improved and have a bright future in real-time monitoring of $PM_{2.5}$, avoiding man-make effects.

Acknowledgements

This work was supported by the National Natural Science Foundation of China (No. 11304300) and the National Basic Research Program of China (Nos. 2011CB932801 and 2012CB933702).The authors thank the Key Laboratory of nuclear magnetic resonance in East China Normal University for ^{13}C NMR measurement.

Notes and references

[a]*School of the Gifted Young, University of Science and Technology of China, Hefei, Anhui 230026, China.*

[b]*The Centre of Physical Experiments, University of Science and Technology of China, Hefei, Anhui 230026, China.*

**Corresponding author: zzm@ustc.edu.cn, Tel & Fax: 86-551-63607671 (Prof. & Dr. Zengming Zhang)*

† Electronic Supplementary Information (ESI) available

1 J. H. Seinfeld, S. N. Pandis, *Atmospheric Chemistry and Physics: From Air Pollution to Climate Change, John Wiley,* Hoboken, New York, 1998
2 F. Echalar, P. Artaxo, J. V. Martins, M. Yamasoe, F. Gerab, W Maenhaut, B. Holben, *J. Geophys. Res*., 1998, **103**, 31849–31864
3 W. F. Cooke, C. Liousse, H. Cachier, J. Feichter, *J. Geophys. Res.*, 1999, **104**, 2137–2162
4 M. H. Bergin, G. R. Cass, J. Xu, C. Fang, L. M. Zeng, T. Yu, L. G. Salmon, C.S. Kiang, X. Y. Tang, Y. H. Zhang, W. L. Chameides, *Journal of Geophysical Research.*, 2001, **106**, 17969–17980
5 D.W. Dockery; C. A. Pope, X. Xu, J. D. Spengler, J. H. Ware, M. E. Fay, B. G. Ferris, F. E. Speizer, *New England Journal of Medecine.*, 1993, **329**, 1753-1759
6 X. Du, Y. Wu, L. Fu, S. Wang, S. Zhang, J. Hao, *Atmospheric Environment.*, 2012, **57**, 233-243
7 C. Cao, W. Jiang, B. Wang, J. Fang, J. Lang, G. Tian, J. Jiang, T. Zhu, *Environ. Sci. Technol.*, 2014, **48**, 1499–1507
8 M. Schaap, K. Müller, H. M. ten Brink, *Atmospheric Environment.*, 2002, **36**, 1323–1335
9 S. Guo, M. Hu, Q. Guo, X. Zhang, M. Zheng, J. Zheng, C. C. Chang, J. J. Schauer, R. Zhang, *Environ. Sci. Technol.*, 2012, **46**, 9846–9853
10 L. Yang, S. Cheng, X. Wang, W. Nie, P. Xu, X. Gao, C. Yuan, W. Wang, *Atmospheric Environment.*, 2013, **75**, 265-269
11 K. He, F. Yang, Y. Ma, Q. Zhang, X. Yao, C. K. Chan, S. Cadle, T. Chan, P. Mulawa, *Atmospheric Environment.*, 2001, **38**, 4959–4970
12 X. Yao, A.P.S. Lau, M. Fang, C. K. Chan, M. Hu, *Atmospheric Environment.*, 2003, **37**, 2991–3000
13 M. Dan, G. Zhuang, X. Li, H. Tao, Y. Zhuang, *Atmospheric Environment.*, 2004, **38**, 3343–3352
14 F. Duan, X. Liu, T. Yu, H. Cachier, *Atmospheric Environment.*, 2004, **38**, 1275–1282
15 M. Zheng, L.G. Salmon, J. J. Schauer, L. Zeng, C. S. Kiang, Y. Zhang, G. R. Cass, *Atmospheric Environment.*, 2005, **39**, 3967–3976
16 Y. Song, X. Xie, Y. Zhang, L. Zeng, L. Salmon, M. Zheng, *Science of the Total Environment.*, 2006, **372**, 278-286
17 Y. Sun Y, G. Zhuang, A. Tang, Y. Wang, Z. An, *Environ. Sci. Technol.*, 2006, **40**, 3148-3155
18 Y. Song Y, X. Tang, S. Xie, Y. Zhang, Y. Wei, M. Zhang, L. Zeng, S. Lu, *Journal of Hazardous Materials.*, 2007, **146**, 124-130
19 Y. Cheng, F. Duan, K. He, M. Zheng, Z. Du, Y. Ma, J. Tan, *Environ. Sci. Technol.*, 2011, **45**, 10117-10123
20 S. Guo, M. Hu, Z. B. Wang, J. Slanina, Y. L. Zhao, *Atmos Chem Phys.*, 2010, **10 (3)**, 947−959
21 M. J. Kleeman, G. R. Cass, *Atmospheric Environment.*, 1998, **32**, 2803-2816
22 S. Squizzato, M. Masiol, F. Visin, A. Canal, G. Rampazzo, B. Pavoni, *Environmental Science: Processes & Impacts*, 2014, **16**, 1913-1922
23 U. Kirchner, R. Vogt, C. Natzeck, J. Goschnick, *Journal of Aerosol Science.*, 2003, **34**, 1323-1346
24 A. Sadezky, H. Muckenhuber, H. Grothe, R. Niessner, U. Poschl, *Carbon.*, 2005, **43**, 1731-742
25 N. P. Ivleva, A. Messerer, X. Yang, R. Niessner, U. Posghl, *Environ. Sci. Technol.*, 2007, **41**, 3702-3707
26 J. C. Chow, P. Doraiswamy, J. G. Watson, L.W.A. Chen, S. S. H. Ho, D. A. Sodeman, *J. Air Waste Manage.*, 2008, **58**, 141-163
27 B. J. Turpin B.J, P. Saxena, E. Andrews, *Atmos. Environ.*, 2000, **34**, 2983-3013
28 E. A. Bruns, V. Perraud, A. Zelenyuk, M. J. Ezell, S. N. Johnson, Y. Yu, D. Imre, B. J. Finlayson-Pitts, M. L. Alexander, *Environ. Sci. Technol.*, 2010, **44**, 1056-1061
29 A. J. Simpson, J. M. Simpson, N. Senesi, B. Xing, P.M. Huang (eds.) *Biophysico-chemical Processes Involving Natural Nonliving Organic Matter in Environmental Systems, John Wiley & Sons,* Hoboken, NJ, 2009, pp. 589-651
30 Y. Subbalakshmi, A. F. Patti, G. S. H. Lee, M. A. Hooper, *J. Environ. Monit.*, 2000, **2**, 561-565
31 Z. Bacsik Z, J. Mink, G. Keresztur, *Appl. Spectrosc. Rev.,* **40**, 327–390
32 A. Polidori, B. J. Turpin, C. I. Davidson, L. A. Rodenburg, F. Maimone, *Aerosol Science and Technology*., 2008, **42**, 233–246
33 H. Rosen, T. Novakov, *Nature.*, 1977, **266**, 706-710
34 J. J. Blaha, G. J. Rosasco, E. S. Etz, *Applied Spectroscopy.*, 1978, **32**, 292-297

35 Health Effects Institute (HEI), *Special Report 15.*, Health Effects Institute, Boston, MA, 2004
36 China Statistical Yearbook, *China Statistics Press.*, Beijing, 2005
37 T. Okuda, J. Kato, J. Mori, *Science of Total Environment.*, 2004, **330**, 145-158
38 J. Zhang, J. Sun, L. An, W. Wang, G. Wang, J. Jin, *Weather Forecast Review.*, 2013, **5**, 51-57 (in Chinese)
39 L. Tumolva, J-Y. Park, J-S. Kim, A. L. Miller, J. C. Chow, J. G. Watson, K. Park, *Aerosol Sci. Tech.*, 2010, **44**, 202-215
40 K. L. Plathe, F. Kammer, M. Hassello et al. *Geochimicaet Cosmochimica Acta* ., 2013, **102**, 213-225
41 B. R. T. Simoneit, *Intern. J. Environ. Anal. Chem.*, 1985, **22**, 203-233
42 E. S. Etz, G. J. Rosasco, J. J. Blaha, *Plenum Publishing Corp.*, 1978, p.413
43 T. Chen, H. Xu, *Acta Petrologica et Mineralogica*, 2003, **4**, 425-428 (in Chinese)
44 T. Okuda, J. Kato, J. Mori, *Science of Total Environment,* 2004, **330**, 145-158
45 S. V. Vassilev, C. G. Vassileva, *Fuel Processing Technology.,* 1996, **47**, 261- 280.
46 S. S. Potgieter-Vermaak S.S, J. H. Potgieter, R. A. Kruger, Z. Spolnika, R. van Grieken, *Fuel.*, 2005, **84** , 2295-2300.
47 J. A. Baldock, J. O. Skjemstad, *Organic Geochemistry.*, 2000, **31**, 697-710
48 A. J. Simpson, M. J. Simpson, R. Soong, *Environ. Sci. Technol.*, 2012, **46**, 11488-11496
49 P. G. Hatcher, D. L. VanderHart, W. L. Earl, *Org. Geochemistry.*, 1980, **2**, 87-92
50 L.P. Lindeman, J. Q. Adams, *Anal. Chem.*, 1971, **43**, 1245-1252
51 J. Mao, X. Fang, Y. Lan, A. Schimmelmann, M. Mastalerz, L. Xu, K. Schmidt-Rohr, *Geochimica et Cosmochimica Acta.*, 2010, **74**, 2110-2127
52 M. W. I. Schmidt, H. Knicker, P. Q. Hatcher, I. Kogel-Knabner, *J. Environ. Qual.*, 2000, **29**, 768-777
53 P. Q. Hatcher, I. A. Breger, *American Chemical Society, Division of Fuel Chemistry.*, Preprints, 1982, **27**, 172-183
54 A. Gelencsér, *Atmos. Oceanogr. Sci. Libr.*, Springer, Dordrecht, Netherlands.2004, **30**, 350pp
55 C. Coury, A. M. Dillner, *Atmospheric Environment.*, 2008, **41**, 9309-9323
56 A. Polidori, B. J. Turpin, C. I. Davidson, L. A. Rodenburg, F. Maimone, *Aerosol Science and Technology.*, 2008, **42**, 233-246
57 N. H. P. Purba, J. Lambert, D. Klockow, *Journal of Amtospheric Chemistry.*, 1998, **29**, 45-54
58 H. Wu, M. Chan, C. Chan, *Aerosol Science and Technology*, 2007, **41**, 581-588
59 R. Huang, Y. Zhang, C. Bozzetti, K. Ho, J. Cao, Y. Han, K. R. Daellenbach, Jay G. Slowik, S. M. Platt, F. Canonaco, P. Zotter, R. Wolf, S. M. Pieber, E. A. Bruns, M. Crippa, G. Ciarelli, A. Piazzalunga, M. Schwikowski, G. Abbaszade, J. Schnelle-Kreis, R. Zimmermann, Z. An, S. Szidat, U. Baltensperger, I. Haddad and A. S. H. Prévôt, *Nature.*, 2014, **514**, 218–222
60 V. C. Farmer, *The infrared spectra of minerals, Mineralogical Society Monograph 4,* Mineralogical Society., London, 1974
61 S. K. Verma, M. K. Deb, *Talanta.*, 2007, **71**, 1546–1552
62 P. C. Painter, R. W. Snyder, M. Starsinic, M. M. Coleman, D. W. Kuehn, A. Davis, *Applied Spectroscopy.*, 1981, **35**, 475-485
63 M. P. Nelson, C. T. Zugates C.T, P. J. Treado, G. S. Gasuccio, D. L. Exline, S. F. Schlaegle, *Aerosol Science and Technology.*, 2001, **34**, 108-117
64 S-K. Sze, N. Siddique, J. J. Sloan, R. Escribano, *Atmospheric Environment.*, 2001, **35**, 561-568
65 J. J. Blaha, G. J. Rosasco, E. S. Etz, *Applied Spectroscopy.*, 1978, **32**, 292-297
66 W. Schumacher, M. Kuhnert, P. Rosch, J. Popp, *J. Raman Spectrosc.*, 2011, **42**, 383-392
67 R. Zhang, J. Jing, J. Tao, S-C. Hsu, G. Wang, J. Cao, C. S. L. Lee, L. Zhu, Z. Chen, Y. Zhao, *Atmospheric Chemistry and Physics.*, 2013, **13**, 7053-7074
68 S. Das, M. J. Hendry, *Chemical Geology.*, 2011, **290**, 101-108
69 X. Wang, J. Li, Q. Zhong, Y. Zhong, M. Zhao, *Journal of Nanomaterials.*, 2013, 101765, 1-6
70 B. Dippel, H. Jander, J. Heintzenberg, *Phys. Chem. Chem. Phys.*, 1999, **1**, 4707-47012
71 A. C. Ferraii, J. Robertson, *Physical Review B.*, 2001, **64**, 075414, 1-13
72 O. Beyssac, B. Goffe, J. P. Petitet, E. Froigenux, M. Moreau, J. N. Rouzaud, *Spectro. chim Acta Part A*, 2003, **59**, 2267-2276
73 Q. Yao, S. Li, H. Xu, J. Zhuo, Q. Song, *Energy.*, 2009, **34**, 1296–1309